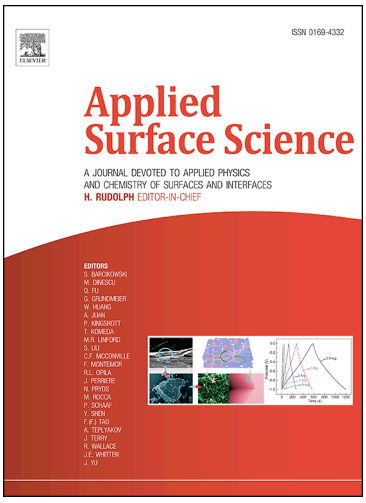

Full Length Article

Copper Nanoparticles synthesis in Hybrid Mesoporous Thin Films: Controlling Oxidation State and Catalytic Performance through Pore Chemistry

Rusbel Coneo Rodríguez, Luis Yate, Emerson Coy, Ángel M. Martínez-Villacorta, Andrea V. Bordoni, Sergio Moya, Paula C. Angelomé

PII: S0169-4332(18)33397-X
DOI: https://doi.org/10.1016/j.apsusc.2018.12.068
Reference: APSUSC 41165

To appear in: *Applied Surface Science*

Received Date: 7 November 2018
Revised Date: 4 December 2018
Accepted Date: 8 December 2018

Please cite this article as: R. Coneo Rodríguez, L. Yate, E. Coy, A.M. Martínez-Villacorta, A.V. Bordoni, S. Moya, P.C. Angelomé, Copper Nanoparticles synthesis in Hybrid Mesoporous Thin Films: Controlling Oxidation State and Catalytic Performance through Pore Chemistry, *Applied Surface Science* (2018), doi: https://doi.org/10.1016/j.apsusc.2018.12.068

Copper Nanoparticles synthesis in Hybrid Mesoporous Thin Films: Controlling Oxidation State and Catalytic Performance through Pore Chemistry

Rusbel Coneo Rodríguez[a], Luis Yate[b], Emerson Coy[c], Ángel M. Martínez-Villacorta[b], Andrea V. Bordoni[a], Sergio Moya[b], Paula C. Angelomé[a]*

(a) Gerencia Química e Instituto de Nanociencia y Nanotecnología – Centro Atómico Constituyentes, Comisión Nacional de Energía Atómica, CONICET, Av. Gral. Paz 1499, B1650KNA San Martín, Buenos Aires, Argentina

(b) CIC biomaGUNE, Paseo de Miramón 182, 20014 Donostia-San Sebastián, Spain

(c) NanoBioMedical Centre, Adam Mickiewicz University, Umultowska 85, 61-614 Poznań, Poland

* Corresponding author email angelome@cnea.gov.ar, telephone: +541167727958

ABSTRACT

The room temperature synthesis of copper (Cu) nanoparticles (NPs) supported within SiO_2 mesoporous thin films (MTF) modified with either COOH or NH_2 functional groups is reported. The functional groups present in the MTF surface acted as adsorption sites for Cu (II) ions, which were afterwards reduced to Cu NPs in presence of sodium borohydride at room temperature. The oxidation state of the copper NPs, corroborated by X-ray Photoelectron Spectroscopy and Electron Energy Loss Spectroscopy, was strongly dependent on the functional group present in the pores of the MTF and on the number of adsorption/reduction (A/R) cycles applied for NPs loading. Metallic Cu (0) NPs were obtained in MTFs displaying COOH groups applying 10 A/R cycles while NPs with higher oxidation state were as well present after 20 A/R cycles. For MTF functionalized with NH_2 groups the copper is present as Cu (I) and Cu(II) in the NPs but no Cu (0) can be detected. The MTF-Cu(CuOx) composite materials were tested as catalysts for the reduction of 4-nitrophenol in the presence of $NaBH_4$. Catalytic activity of composite materials depends on the oxidation state of Cu NPs, being more active those samples containing Cu (0) NPs, synthesized from COOH functionalized MTFs.

KEYWORDS

Copper nanoparticles; copper oxide; mesoporous thin films; functionalized nanopores; hybrid materials; catalysts.

INTRODUCTION

Metallic nanoparticles (NPs) have interesting size-dependent optical and catalytic properties and a high surface to volume ratio that make them appealing for many different applications, such as sensing, catalysis, energy conversion and storage, biomedicine and environmental technology, to cite a fews.[1],[2] Among the various metal NPs, Au and Ag NPs are the most frequently used for optical applications and Pt and Pd NPs are the most appealing for catalysis.

In recent years, copper NPs have also received increasing attention for their excellent performance in electronics, sensing and catalysis.[3],[4] Cu has multiple advantages: it is abundant, it can catalyze a great variety of reactions[5] and it is an inexpensive metal.[6] However, the susceptibility of Cu (0) to oxidation upon exposure to air represents a big challenge for the synthesis of metallic Cu NPs Therefore, literature on Cu NPs is rather limited compared with other metallic NPs.[7]

Cu displays multiple oxidation states and usually forms two stable oxides: Cu_2O and CuO.[8] In particular, Cu_2O is an environmentally friendly *p*-type semiconductor with a band gap of 2 eV and high optical absorption coefficient, which makes it an excellent candidate for solar-energy-conversion applications.[8] This range of accessible oxidation states results in a reactivity involving the exchange of one or two electron. Because of this versatility, Cu oxides can promote a variety of reactions.[1] For example both Cu (I) and Cu (II) oxides have been reported to have catalytic activity for azide alkyne cycloaddition (CuAAC) reactions[9],[10], 4-nitrophenol (4-NIP) reduction[11] and tryazoles synthesis.[12]

Both Cu and CuOx NPs synthesized in solution require stabilization in order to avoid nanoparticle coarsening and/or aggregation. The use of porous templates has become one of the most promising strategies for NPs support and stabilization.[1, 13] In particular, ordered mesoporous oxides are highly appealing supports due to their high specific area and, in the case of transition metal based oxides, for their good stability in reaction media. The use of mesoporous oxides as supports for metallic or Cu NPs can improve the selectivity, conversion and yield of Cu(CuOx) catalyzed reactions and, most important, the mesoporous oxide will facilitate the recovery of the catalysts.[1, 13, 14] Several syntheses of powdered mesoporous materials modified with Cu(CuOx) NPs have been reported in the literature.[15-28] In most of those cases, Cu (II) is first adsorbed to

the mesoporous surface through surface functionalization, and then a thermal treatment follows that results in the NPs formation. The Cu(CuOx) mesoporous composite powders have been mainly applied on catalysis of organic reactions. The use of mesoporous thin films (MTF) instead of powders as supports for Cu based catalysts will result in more efficient recovery and reuse than in the case of powdered supports and can also facilitate the integration of the catalyst in devices.[29-31] However, up to now only Ag, Au and Pt loaded MTF have been synthesized and used as catalysts and no examples can be found in the literature about Cu loaded MTF synthesis and/or applications.

In this work, we have explored the room temperature synthesis of Cu based NPs supported within SiO_2 MTF. This silica based MTF present the typical properties of mesoporous oxides, including: high surface area, ordered porosity and versatility for organic functionalization during or after the materials' synthesis.[31, 32] The pores in silica MTF can be easily modified including silanes during its synthesis. This allows good control of the chemistry of the pore and the functional groups present within. Profiting from this advantage pores were modified with either COOH or NH_2 functional groups. Both COOH and NH_2 can act as adsorption sites for Cu (II).[33] However, it will be shown that the choice of one or the other group will finally determine the oxidation state of the resulting NPs. The MTF-Cu(CuOx) composite materials were tested as catalysts for the reduction of 4-nitrophenol in the presence of $NaBH_4$. Catalytic activity depends on the Cu NPs oxidation state, which was in turn determined by the functional group included within the oxide used as support.

To resume, here we will show that it is possible to control the formation of metallic or metal oxide Cu NPs in mesoporous materials by varying the chemistry of the pore. This opens the route for the design of hybrid SiO_2 MTF including *in situ* synthesized metal or metal oxide NPs with controlled chemistry and properties.

MATERIALS AND METHODS

a) Materials

Tetraethyl orthosilicate (TEOS, 98%), vinyltrimethoxysilane (VTMS, 98%), mercaptoacetic acid (MAA, 97%), benzophenone (Ph_2CO, 99%), Pluronic F127, hydrochloric acid (37%), methanol, $CuSO_4.5H_2O$, NaOH, aminopropyltriethoxysilane (APTES), sodium borohydride, ascorbic acid and 4-

nitrophenol (4-NIP) were obtained from Merck. Methanol, pure grade ethanol and Milli-Q water were used as solvents. Methanol was dried over activated MS-3 Å before use.

b) Synthesis of hybrid SiO_2 MTF

b.1) Synthesis of carboxylic trialkoxysilane precursor by click reaction

2-((2-(trimethoxysilyl)ethyl)thio)acetic acid ($(MeO)_3$Si-MAA) was prepared as previously reported.[34] Briefly, 2.86 mmol of VTMS was added to a vial containing 1 mL of a methanol solution of MAA (2.86 mmol) and 15% mol of Ph_2CO as photoinitiator. The solution was irradiated for 16 h, under gentle stirring, using a 15 W black-light lamp (λ_{max} = 360 nm). The amount of modified silane was chosen to have a final concentration of 20% of the organic function in the preparation of the sol. The reaction mixture was used for the subsequent step, without any additional treatment.

b.2) Preparation of sols

Hybrid sols for synthesis of functionalized mesoporous films were prepared by first mixing TEOS, ethanol and Pluronic F127. Then, the functional silane was added dropwise under stirring. For COOH modified films, the reaction mixture of click reaction was used; and for NH_2 modified films, APTES was chosen as the precursor.[35] Finally, an HCl solution was added dropwise under stirring. The chosen order of mixture results in stable solutions that can be kept in the freezer for several months. The molar proportions of the sols were TEOS : Si-R : F127 : HCl : EtOH : H_2O = 0.8 : 0.2 : 0.005 : 0.28 : 24 : 5.2, with Si-R = $(MeO)_3$Si-MAA or $(EtO)_3$Si-NH_2. After preparation the sol was aged for 1 h before use.

b.3) Preparation of films

Functionalized mesoporous thin films were produced by combining sol–gel reactions with self-assembly of amphiphilic molecules, through the strategy known as Evaporation Induced Self Assembly.[36] The resulting sols were used to produce films by dip-coating on carefully cleaned glass substrates, under 40–50% relative humidity at 25 °C, using 2 mm s^{-1} withdrawing speed. Freshly deposited films were placed in a chamber with a 50% relative humidity for 24 h at 25 °C, followed by a stabilizing thermal treatment of two successive 24 h steps at 60 °C and 130 °C, and a final 2 h step at 200 °C. The template was extracted by immersing the films for 2 days in ethanol.

c) Synthesis of Cu based NPs inside the films

Cu NPs supported into mesoporous films were synthesized by a chemical reduction method that involves the reaction of Cu (II) with sodium borohydride, following a procedure proposed for NPs synthesis in solution.[37] For that purpose, 25 mL of 0.01 M $CuSO_4 \cdot 5H_2O$ solution was prepared in deionized water; 0.5 ml of 0.03 M ascorbic acid solution was slowly added and under stirring, followed by the addition of 80 µl of 1 M NaOH solution.

The formation of Cu NPs into mesoporous films was achieved by iterative Cu adsorption/reduction (A/R) cycles, represented in Scheme 1. Films were first immersed for 30 min in the Cu (II) solution, then were extracted and carefully rinsed with Milli-Q water. Then, films were immersed for 3 min in a 10 mM $NaBH_4$ solution, rinsed with water and dried under N_2 flow. These two consecutive steps were repeated 10 and 20 times. Depending on the functional group used and the number of cycles applied samples are denominated SiO_2-COOH-Cu_x or SiO_2-NH_2-Cu_x, where *x* is the number of A/R cycles.

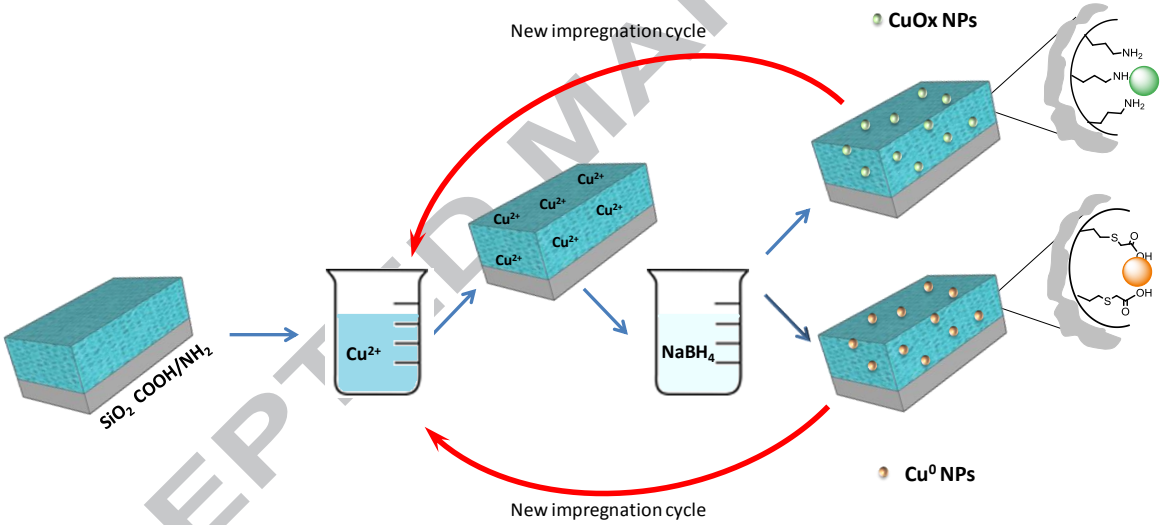

Scheme 1. Schematic representation of the synthetic method used to produce Cu NPs in MTF pores functionalized with COOH and NH_2 groups.

d) Characterization

UV-vis absorption spectra were measured with a Cary 5000 UV-vis-NIR spectrophotometer (Varian, Inc.).

Transmission electron microscopy (TEM) images were obtained with a JEOL JEM-2100F UHR operated at 200 kV. High Resolution TEM (HR-TEM) images and electron energy loss spectra (EELS) were acquired with a JEOL – ARM200F (200kV) equipped with a field emission gun and a Gatan GIF

quantum EELS spectrometer. Samples were measured immediately after scratching the glass surfaces and casting the collected dust on membrane-free lacey carbon grids (Ted Pella).

X-ray photoelectron spectroscopy (XPS) measurements were carried out with a SPECS Sage HR 100 spectrometer equipped with a 100 mm mean radius PHOIBOS analyzer and a non-monochromatic X-ray source (Mg Kα line of 1253.6 eV energy and 250 W), placed perpendicular to the analyzer axis and calibrated using the $3d_{5/2}$ line of Ag, with a full width at half maximum of 1.1 eV. The selected resolution for high resolution spectra was 15 eV of pass energy and 0.15 eV per step. All measurements were made in an ultrahigh vacuum chamber at a pressure of around 8×10^{-8} mbar. An electron flood gun was used to neutralize for charging. Measurements were conducted directly on the films, which were previously washed with absolute ethanol and cut into samples of 1 cm × 1 cm.

e) Catalytic activity

The well-known reduction of 4-NIP by $NaBH_4$ was used as model reaction to study the catalytic activity of the obtained composites. For that purpose, 10 µL of 4-NIP 0.01 M solution and 100 µL of freshly prepared $NaBH_4$ 0.5 M solution were mixed with 2.5 ml of milliQ water. A piece of ~1 cm^2 of the MTF catalyst was introduced in a 3 mL quartz cuvette filled with the reaction solution. The slide was positioned inside the cuvette in such way that it did not block the beam path. The reaction was followed using the spectrophotometer described before. The absorbance of the solution was recorded in the 200–800 nm range every 5 minutes until reaction completion.

Copper content of the composites used for catalytic tests was measured by inductively coupled plasma mass spectrometry (ICP-MS). For this purpose, pieces of ~ 2.25 cm^2 of the same samples used for catalysis tests were immersed in boiling HNO_3 (c) and refluxed during 1 hour. Then, the remaining piece of substrate was removed and the solution was boiled for some minutes to concentrate it. Finally, the 0.25 mL of the digestion was mixed with 2.75 mL of milliQ water and this solution was used to carry out the measurements.

RESULTS AND DISCUSSION

SYNTHESIS AND STRUCTURAL CHARACTERIZATION

Copper NPs were synthesized inside SiO_2 MTF functionalized with carboxylic acid (SiO_2–COOH) or amine groups (SiO_2–NH_2) through Cu (II) adsorption followed by a chemical reduction at room temperature. MTFs were synthesized according to previously reported procedures[34, 35] that

result in thin films of around 200 nm thickness, and 30% of porosity. In both cases, Pluronic F127 was used as template for the pore formation and, as a consequence, both kinds of films present a well-ordered mesoporous body centered cubic (*Im3m*) structure with a pore's periodicity of 8.5 nm. The method used to deposit Cu NPs inside the films is based on the combination of a previously reported procedure for the synthesis of Au nanoparticles inside mesoporous thin films [38, 39] and a method for obtaining Cu NPs in solution.[37] In the first step, the Cu (II) species present in the solution are adsorbed into the MTF, taking advantage on the presence of functional groups (COOH or NH_2) that can complex the metallic ions. Remarkably, the use of ascorbic acid and NaOH mixture in the metal salt solution allows better results in this adsorption step, due to the fact that the pH is higher than when only Cu (II) is used (5.6 vs 4.9). The second step involves the reduction of the previously adsorbed Cu (II) species by BH_4^-, a well-known reductive agent. Since the amount of Cu (II) that can be adsorbed by the MTF in each step is limited, the adsorption-reduction cycles are repeated several times in order to ensure the formation of an adequate amount of NPs, as depicted in Scheme 1.

Figure 1**Figure** shows the TEM images of the resulting composite materials. As shown in Figure 1a, Cu structures are clearly visible in the pores since highly dense materials, like metallic particles, are seen as dark spots in transmission electron images. Conversely, in dark field images (see Figure S1, SI), the high density materials can be visualized as bright objects.

The in pore synthesized NPs are spherical and have an average diameter of ~3.8 nm and ~3.5 nm for SiO_2–COOH-Cu_{10} and SiO_2–NH_2-Cu_{10} samples, respectively. It is interesting to mention that in the case of the SiO_2–COOH-Cu_{20} sample, *i.e*. the one in which the A/R cycles were repeated 20 times, the NPs size is ~3.9 nm, similar to the size of the other samples prepared with 10 cycles, indicating that the NPs size is controlled by the pore size (5 nm of diameter, approximately).[34] While a larger number of A/R cycles does not imply an increase in the NPs size, the amount of Cu incorporated inside the films increases, as demonstrated by XPS measurements (see Table 1). This means that more pores are filled with NPs. It is interesting to note, however, that the relation between number of A/R cycles and amount of Cu incorporated is not linear, as observed previously for Au NPs incorporation within mesoporous TiO_2.[39] This is probably due to differences in the amount of Cu (II) species that can be adsorbed in already filled pores.

After NP synthesis samples show color changes, being brown for SiO_2-COOH-Cu_{10} and green for SiO_2-COOH-Cu_{20} (see Figure S2, SI). These differences in color, observed by naked eye, suggests the

presence of Cu NPs for the SiO_2-COOH-Cu_{10} samples, while the SiO_2-COOH-Cu_{20} should be loaded with copper oxide (CuOx) NPs or a mixture of both.[8]

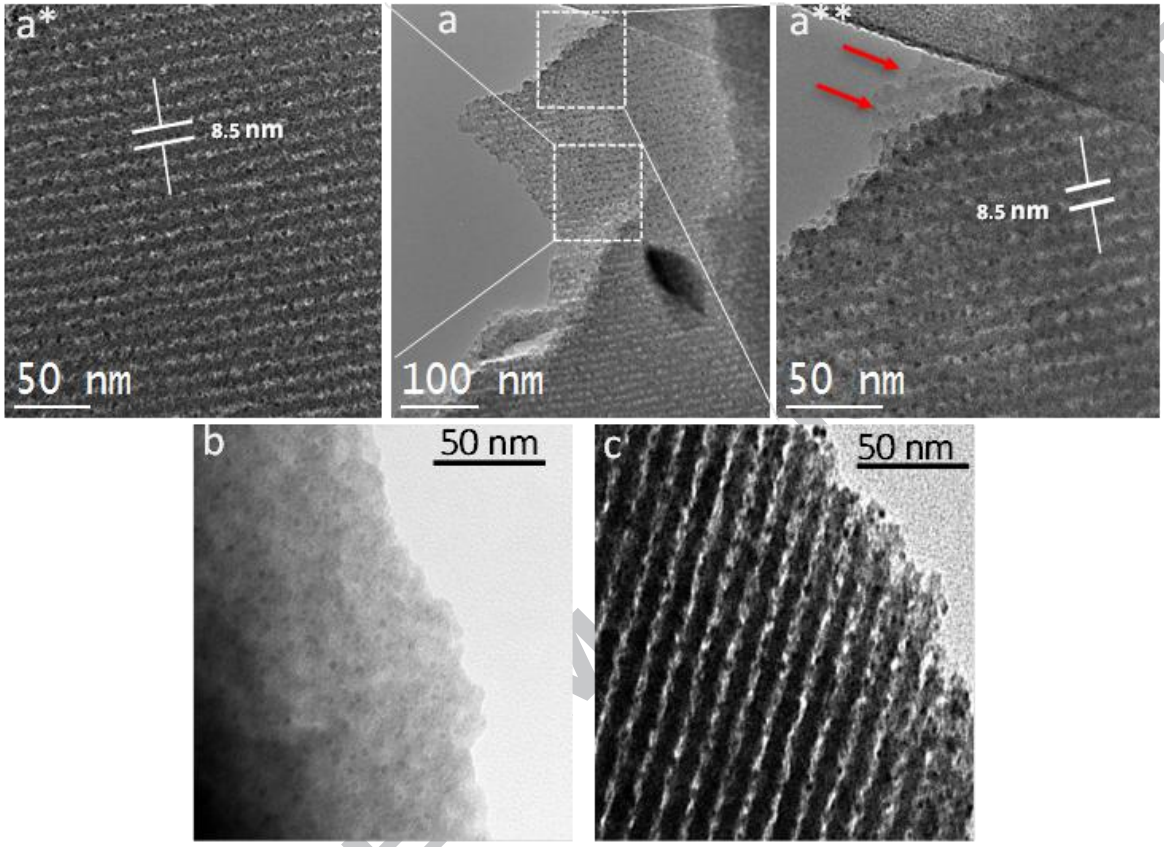

Figure 1. TEM micrographs of (a, a* and a**) SiO_2–COOH-Cu_{10}, under different magnifications, (b) SiO_2-NH_2-Cu_{10} and (c) SiO_2-COOH-Cu_{20} samples.

Table 1. Cu/Si % obtained by XPS

Sample	***Cu/Si (%)***
SiO_2-COOH-Cu_{10}	2.69
SiO_2-COOH-Cu_{20}	9.46
SiO_2-NH_2-Cu_{10}	3.09

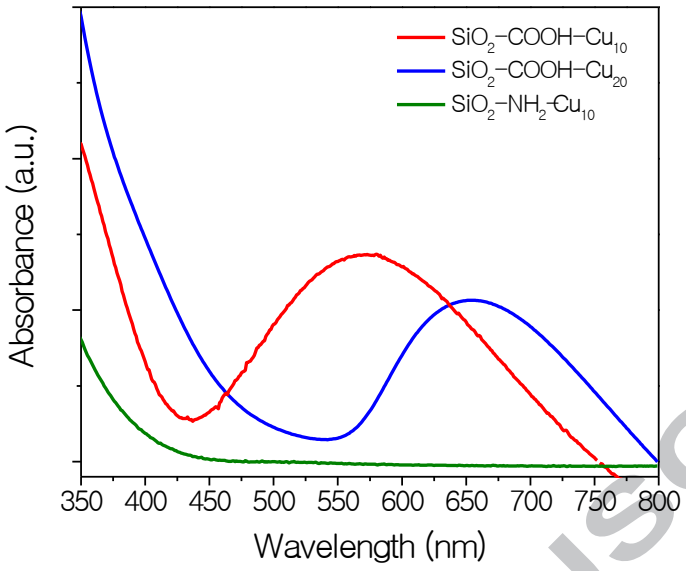

Figure 2. UV–vis spectra SiO_2-COOH-Cu_{10}, SiO_2-COOH-Cu_{20} and SiO_2-NH_2-Cu_{10} samples, as indicated in the labels.

Figure 2 shows the UV –Vis spectra of the MTF Cu composites. A localized surface plasmon resonance (LSPR) band between 570 and 600 nm is observed for the SiO_2-COOH-Cu_{10} sample.[40] Spherical Cu (0) nanoparticles synthesized in solution display an LSPR band centered at 570 nm.[41-43] However, the exact location of this LSPR maximum depends on the particle size, aspect ratio, capping agent and the average dielectric constant of the surrounding environment.[43] Thus, the band observed for SiO_2-COOH-Cu_{10} can be attributed to Cu (0) and the broadness of the band is probably related to the NPs size distribution. Moreover, the LSPR band for the SiO_2-COOH-Cu_{10} sample remains almost invariable for at least 8 days, hinting that the Cu NPs are stable in the MTF and protected from air oxidation (see Figure S3, SI).

SiO_2-COOH-Cu_{20}, on the other hand, presents a UV-vis band that is shifted towards longer wavelength, with a maximum around 650 nm. Also, a small attenuation in the intensity of the plasmon was observed. The observed shift could be associated to changes in the oxidation state of the NPs surface, when the amount of A/R cycles is increased. In particular, the presence of semiconductor Cu_2O can contribute in two ways to the observed red-shift: due to the increment on the local refractive index around the Cu (0)[44] and due to the appearance of an excitonic band.[45, 46] Moreover, it is important to note that surface oxidation of many metals occurs at a

rapid rate until the formation of an oxide layer passivates the surface and prevents its total oxidation.[8]

For the SiO_2-NH_2-Cu_{10} sample the LSPR resonance band attributed to Cu (0) NPs and/or Cu (I) oxide were not observed. The absence of the LSPR or excitonic bands suggests that the NPs obtained in presence of NH_2 groups display a different oxidation state from the NPs obtained in presence of COOH groups.[47]

In order to evaluate more carefully the oxidation state of the synthesized NPs, samples were characterized by XPS measurements. XPS spectra of SiO_2-COOH-Cu_{10} and SiO_2-COOH-Cu_{20} samples are presented in Figure 3.

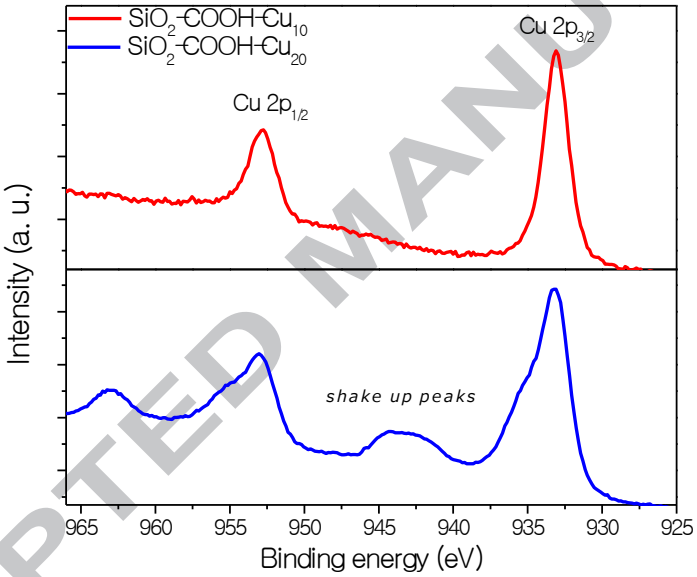

Figure 3. XPS spectra of SiO_2-COOH-Cu_{10} and SiO_2-COOH-Cu_{20} samples in the Cu region, as indicated in the labels.

For both samples, the XPS spectra feature Cu 2p peaks, which confirm the incorporation of Cu inside the mesoporous structure. Interestingly, the shape of the spectra depends on the number of A/R cycles used to prepare the sample. For 10 A/R cycles, the spectrum show two peaks: the one corresponding to Cu $2p_{3/2}$ around 933 eV and the one of Cu $2p_{1/2}$ at around 952 eV. According to previously reported data,[48] the presence of such peaks indicate the presence of Cu (0) and/or Cu (I) species. The two species cannot be easily distinguished by XPS analysis. For the SiO_2-COOH-

Cu_{20} sample, Cu $2p_{1/2}$ and Cu $2p_{3/2}$ peaks are again present, and both peaks are less symmetric than for 10 A/R cycles displaying shoulder peaks pointing towards the presence of Cu (II) species, whose XPS peaks appear at higher binding energies.[48] Moreover, the characteristic shake-up peaks of Cu(II) species between 945 and 940 eV can be clearly seen in the 20 A/R cycles sample. Since these signals are exclusive of Cu (II) species[48] we can conclude from XPS results that the oxidation state of Cu NPs depends on the number of A/R cycles used for its synthesis inside the mesoporous film.

Since XPS results were not conclusive regarding the Cu species identification, EELS measurement were performed, in order to clarify this point. Results are presented in Figure 4.

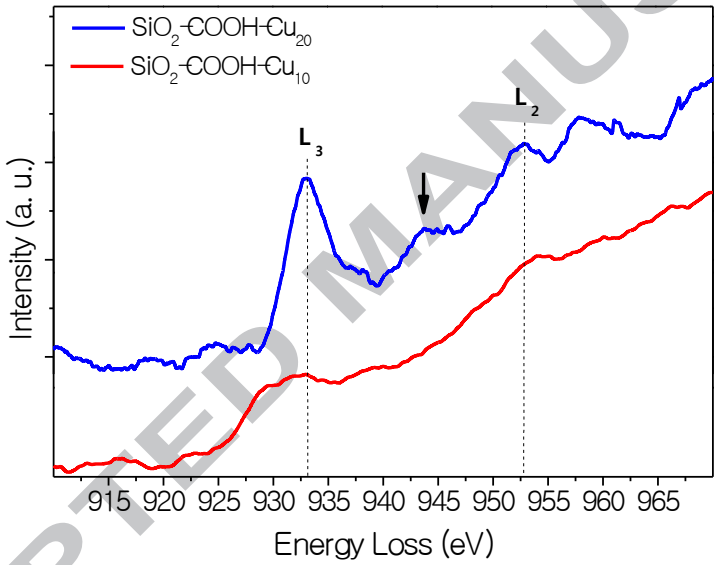

Figure 4. Cu $L_{2,3}$ edge EELS spectra for SiO_2-COOH-Cu_{10} and SiO_2- COOH-Cu_{20} samples, as indicated in the labels.

The background subtracted EELS spectra, denominated energy loss near edge structure (ELNES), show the Cu $L_{2,3}$ edge due to the excitation from the occupied 2p core shell to the vacant 3d states localized at Cu NPs. The SiO_2-COOH-Cu_{10} sample spectrum shows flat and broad $L_{2,3}$ edges, which correspond to metallic Cu and the SiO_2-COOH-Cu_{20} sample spectrum shows peaks attributed at the $L_{2,3}$ edge.[49] Also, an extra peak located at 947.5 eV can be observed for the sample prepared with 20 A/R cycles; this peak could be attributed to the transitions into the 4s Cu states above the Fermi level,[50] which is associated to the presence of Cu (I), Cu (II) or a mixture of both.[40]

By analyzing XPS and EELS results, it can be concluded that COOH groups available in the mesoporous SiO_2 films can be used as an effective support to synthesize and stabilize metallic Cu (0) nanoparticles when 10 A/R cycles are applied.[16] However, for 20 A/R cycles this protective effect was not observed, suggesting that it only takes place until a particular Cu/COOH ratio, and increasing the Cu concentration the carboxylic groups cannot prevent the oxidation of the metal surface.[51]

The influence of the functional groups present in the pores of SiO_2 MTF on the oxidation state of Cu NPs was also evaluated, by comparing the COOH modified oxides with the samples containing NH_2 groups. The XPS spectrum of the SiO_2-NH_2-Cu_{10} sample is presented in Figure 5.

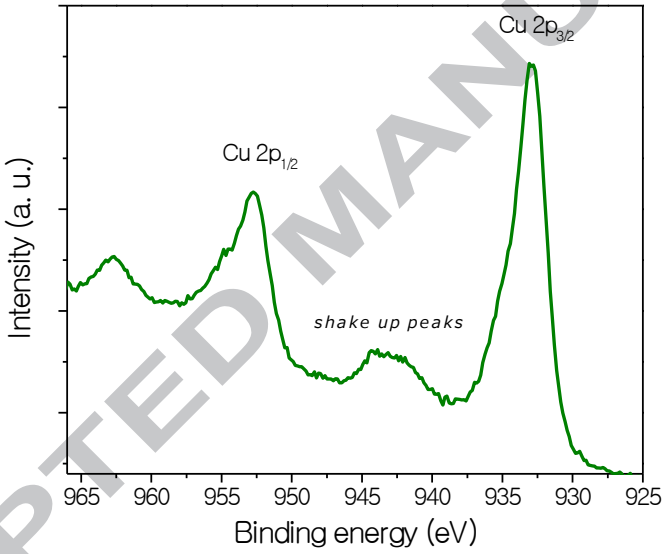

Figure 5. XPS spectrum of the SiO_2-NH_2-Cu_{10} sample.

The spectrum presents similar features to the one of SiO_2-COOH-Cu_{20} sample: Cu $2p_{3/2}$ peaks at binding energies around 932.8 and 935.0 eV and the presence of shake up peaks in the 945-940 eV region. XPS results, together with the absence of absorption bands in UV-visible spectra, point towards the presence of Cu (I) / Cu (II) species inside the amino functionalized mesoporous structure.

These results demonstrate the influence of the pores' surface chemistry over the oxidation states of the obtained Cu NPs. The NH_2 groups allow the adsorption of Cu (II) onto the mesoporous oxide

surface and possibly the Cu (0) NP formation, but the amine groups in the pores seem to not have such a protective effect against the oxidation process that occurs in aerobic conditions, therefore, the Cu (0) species are oxidized.

Catalytic Activity

The catalytic activity of all composites was studied using a well-known model catalytic reaction: the reduction of 4-NIP with $NaBH_4$.[52] Despite being usually taken as model reaction it is important to highlight that this reaction has also practical applications, since 4-NIP is a common pollutant from industrial wastes.[53]

The reaction was performed immersing ~1 cm^2 pieces of each MFT composite in stirred solutions containing the reactants.[54] The reaction was monitored by UV–vis spectroscopy. In all tested cases, a decrease of the 4-NIP absorption band centered at 400 nm and the appearance of a new peak located at 300 nm were observed, indicating the conversion of 4-NIP into 4-aminophenol (see Figure S4, SI).[55] The reaction rate was modeled according to pseudo first-order kinetic that can be described by the following equation:

$$\ln(A_t/A_0) = -kt$$

Where t is the reaction time, A_t and A_0 are the absorbances of 4-NIP at 400 nm at time t and 0, respectively and k is the reaction constant rate.[56],[57] Figure 6 shows the plot of $\ln(A_t/A_0)$ as a function of reaction time for the composites used as catalysts. All data can be linearly fitted, confirming the pseudo first order kinetic assumption.[58]

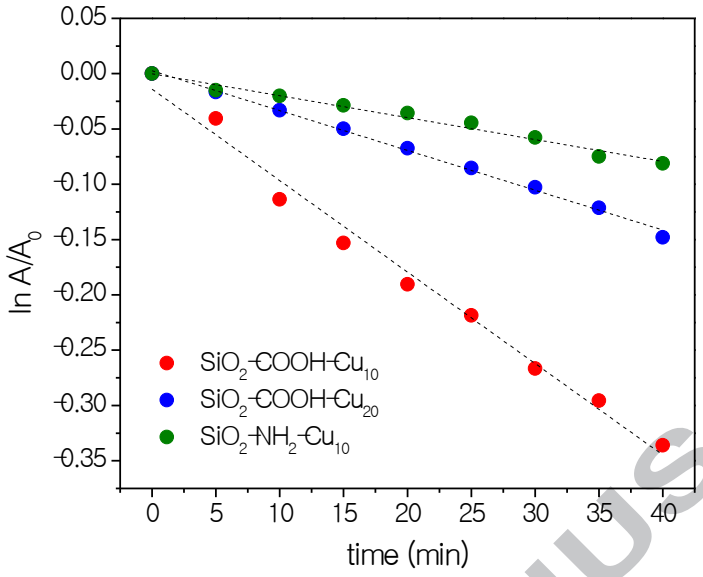

Figure 6. Plot of ln (A_t /A_0) as a function of time for the reaction catalyzed by SiO_2- COOH-Cu_{10}, SiO_2- COOH-Cu_{20} and SiO_2-NH_2-Cu_{10} composite materials.
The lines correspond to linear fitting of the data.

The resulting geometric-area normalized apparent constants rates (k_{app}, obtained taking into account the geometric area of the sample and its Cu content) are presented in Table 2. These k_{app} are in order of values reported in literature for non-supported metallic NPs.[11],[55],[59]

The induction time required for the reaction start was of about 2 minutes for all samples, and can be related with diffusion processes that take place within the mesoporous structure,[60] as observed before for Cu NPs loaded SBA-15 mesoporous catalysts.[53] The obtained values indicate an easy diffusion of the reagents into the mesoporous matrix.[54]

Table 2 Constant rates for the 4-NIP reduction catalyzed by Cu loaded SiO_2 MTF

Sample	k_{app} [10^{-3} min^{-1} cm^{-2}] *	k'_{app} [10^3 min g] $^{-1}$ **
SiO_2-COOH-Cu_{10}	8.3	16.2
SiO_2-COOH-Cu_{20}	3.6	4.2
SiO_2-NH_2-Cu_{10}	2.0	6.8

** normalized per geometric area*
***normalized per Cu content measured by IC-PMS (see Table S1, SI)*

Although all the obtained composite materials present catalytic activity for 4-NIP reduction, the best results in terms of k_{app} were obtained for SiO_2-COOH-Cu_{10} sample, where Cu is present as Cu (0). Indeed the k_{app} has a value of 8.3 10^{-3} $min^{-1}.cm^{-2}$ for the SiO_2-COOH-Cu_{10} sample, more than twice the value for the SiO_2-COOH-Cu_{20} sample and four times the value of the k_{app} of the SiO_2-NH_2-Cu_{10} sample. Moreover, XPS measurements performed after the catalytic measurements demonstrate that Cu (0) remains in the sample after the experiments (see Figure S5, SI), hinting on the chemical stability of the obtained composites.

These results confirms, as expected, that the oxidation state of Cu inside the composite material is a critical point for the control of its catalytic activity. This feature depends not only on the NPs surface to volume ratio and exposed facets, but also on their oxidation state. Interestingly, this last characteristic of the NPs can be controlled through MTF functionalization combined with the number of A/R cycles performed to incorporate the copper.

CONCLUSIONS

Cu NPs were grown inside accessible porous SiO_2 MTF functionalized with COOH and NH_2 groups at room temperature, using an adsorption-reduction procedure based on easily available reagents. The oxidation state of the Cu NPs depended both on the functional group present in the pores and the number of adsorption-reduction steps applied, as demonstrated by UV-visible spectra, XPS and EELS analysis. Metallic Cu (0) NPs were obtained for MTF displaying pores functionalized with COOH groups and applying 10 A/R cycles. For the same pore functionalization, Cu NPs with higher oxidation state were also present when 20 A/R cycles were used. This observation hints a stabilization effect due to the presence of COOH group, is more effective when less Cu is present inside the MTF. When NH_2 groups are present in the pores, on the other hand, Cu (0) is not present in the NPs, indicating a lower stabilizing capacity of the amines.

The oxidation state of Cu NPs controlled the catalytic activity of the composite material towards 4-NIP reduction: the more active samples were the ones that contained Cu (0) NPs. Catalytic activity can be therefore controlled through the proper choice of MTF functionalization combined with the number of A/R cycles performed to incorporate the copper.

Our result show a simple methodology for controlling the chemistry and performance of in pore synthesized nanoparticles by modifying the surface chemistry of the pores. Such approach can be applied for the synthesis of other NPs and it is a nice example of the interplay between pore chemistry and functionality in mesoporous materials.

ACKNOWLEDGEMENTS

This work has been funded by CONICET (PIP 00044CO) and ANPCyT (PICT 2013-1303 and PICT 2015-0351). R.C.R. acknowledges CONICET for a postdoctoral scholarship. Dr. Alberto E. Regazzoni is gratefully acknowledged for his comments during manuscript elaboration.

REFERENCES

[1] M.B. Gawande, A. Goswami, F.-X. Felpin, T. Asefa, X. Huang, R. Silva, X. Zou, R. Zboril, R.S. Varma, Cu and Cu-based nanoparticles: synthesis and applications in catalysis, Chem. Rev., 116 (2016) 3722-3811.
[2] C. Clavero, Plasmon-induced hot-electron generation at nanoparticle/metal-oxide interfaces for photovoltaic and photocatalytic devices, Nature Photonics, 8 (2014) 95.
[3] M. Luo, A. Ruditskiy, H.C. Peng, J. Tao, L. Figueroa-Cosme, Z. He, Y. Xia, Penta-Twinned Copper Nanorods: Facile Synthesis via Seed-Mediated Growth and Their Tunable Plasmonic Properties, Adv. Funct. Mater., 26 (2016) 1209-1216.
[4] X. Liu, J. Ruiz, D. Astruc, Prevention of aerobic oxidation of copper nanoparticles by anti-galvanic alloying: gold versus silver, Chem. Commun., 53 (2017) 11134-11137.
[5] D. Wang, D. Astruc, The recent development of efficient Earth-abundant transition-metal nanocatalysts, Chem. Soc. Rev., 46 (2017) 816-854.
[6] A.S. Preston, R.A. Hughes, T.B. Demille, S. Neretina, Copper Template Design for the Synthesis of Bimetallic Copper–Rhodium Nanoshells through Galvanic Replacement, Part. Part. Syst. Char., (2018).
[7] Y. Xia, Y. Xiong, B. Lim, S.E. Skrabalak, Shape-controlled synthesis of metal nanocrystals: Simple chemistry meets complex physics?, Angew. Chem. Int. Ed., 48 (2009) 60-103.
[8] L.I. Hung, C.K. Tsung, W. Huang, P. Yang, Room-Temperature Formation of Hollow Cu2O Nanoparticles, Adv. Mater., 22 (2010) 1910-1914.
[9] J.E. Hein, V.V. Fokin, Copper-catalyzed azide–alkyne cycloaddition (CuAAC) and beyond: new reactivity of copper (I) acetylides, Chemical Society Reviews, 39 (2010) 1302-1315.
[10] F. Fu, A. Martinez, C. Wang, R. Ciganda, L. Yate, A. Escobar, S. Moya, E. Fouquet, J. Ruiz, D. Astruc, Exposure to air boosts CuAAC reactions catalyzed by PEG-stabilized Cu nanoparticles, Chem. Commun., 53 (2017) 5384-5387.
[11] C. Wang, R. Ciganda, L. Salmon, D. Gregurec, J. Irigoyen, S. Moya, J. Ruiz, D. Astruc, Highly efficient transition metal nanoparticle catalysts in aqueous solutions, Angew. Chem. Int. Ed., 55 (2016) 3091-3095.
[12] Y.-H. Tsai, K. Chanda, Y.-T. Chu, C.-Y. Chiu, M.H. Huang, Direct formation of small Cu2O nanocubes, octahedra, and octapods for efficient synthesis of triazoles, Nanoscale, 6 (2014) 8704-8709.
[13] R.J. White, R. Luque, V.L. Budarin, J.H. Clark, D.J. Macquarrie, Supported metal nanoparticles on porous materials. Methods and applications, Chem. Soc. Rev., 38 (2009) 481-494.

[14] J. Sun, X. Bao, Textural Manipulation of Mesoporous Materials for Hosting of Metallic Nanocatalysts, Chemistry - A European Journal, 14 (2008) 7478-7488.
[15] C.S. Chen, Y.T. Lai, T.W. Lai, J.H. Wu, C.H. Chen, J.F. Lee, H.M. Kao, Formation of Cu Nanoparticles in SBA-15 Functionalized with Carboxylic Acid Groups and Their Application in the Water–Gas Shift Reaction, ACS Catalysis, 3 (2013) 667-677.
[16] C.-S. Chen, C.-C. Chen, C.-T. Chen, H.-M. Kao, Synthesis of Cu nanoparticles in mesoporous silica SBA-15 functionalized with carboxylic acid groups, Chem. Commun., 47 (2011) 2288-2290.
[17] A. Chirieac, B. Dragoi, A. Ungureanu, C. Ciotonea, I. Mazilu, S. Royer, A.S. Mamede, E. Rombi, I. Ferino, E. Dumitriu, Facile synthesis of highly dispersed and thermally stable copper-based nanoparticles supported on SBA-15 occluded with P123 surfactant for catalytic applications, J. Catal., 339 (2016) 270-283.
[18] B. Dragoi, I. Mazilu, A. Chirieac, C. Ciotonea, A. Ungureanu, E. Marceau, E. Dumitriu, S. Royer, Highly dispersed copper (oxide) nanoparticles prepared on SBA-15 partially occluded with the P123 surfactant: toward the design of active hydrogenation catalysts, Catalysis Science & Technology, 7 (2017) 5376-5385.
[19] V.S. Garcia-Cuello, L. Giraldo, J.C. Moreno-Piraján, Synthesis, Characterization, and Application in the CO Oxidation over a Copper Nanocatalyst Confined in SBA-15, Journal of Chemical & Engineering Data, 56 (2011) 1167-1173.
[20] C. Huo, J. Ouyang, H. Yang, CuO nanoparticles encapsulated inside Al-MCM-41 mesoporous materials via direct synthetic route, Scientific Reports, 4 (2014) 3682.
[21] R.J. Kalbasi, A.A. Nourbakhsh, M. Zia, Aerobic Oxidation of Alcohols Catalyzed by Copper Nanoparticle-Polyacrylamide/SBA-15 as Novel Polymer-Inorganic Hybrid, Journal of Inorganic and Organometallic Polymers and Materials, 22 (2012) 536-542.
[22] C.-H. Liu, N.-C. Lai, J.-F. Lee, C.-S. Chen, C.-M. Yang, SBA-15-supported highly dispersed copper catalysts: Vacuum–thermal preparation and catalytic studies in propylene partial oxidation to acrolein, J. Catal., 316 (2014) 231-239.
[23] C. Marras, D. Loche, D. Carta, M.F. Casula, M. Schirru, M.G. Cutrufello, A. Corrias, Copper-Based Catalysts Supported on Highly Porous Silica for the Water Gas Shift Reaction, ChemPlusChem, 81 (2016) 421-432.
[24] C. Rudolf, F. Abi-Ghaida, B. Dragoi, A. Ungureanu, A. Mehdi, E. Dumitriu, An efficient route to prepare highly dispersed metallic copper nanoparticles on ordered mesoporous silica with outstanding activity for hydrogenation reactions, Catalysis Science & Technology, 5 (2015) 3735-3745.
[25] S. Sareen, V. Mutreja, S. Singh, B. Pal, Highly dispersed Au, Ag and Cu nanoparticles in mesoporous SBA-15 for highly selective catalytic reduction of nitroaromatics, RSC Advances, 5 (2015) 184-190.
[26] C.-H. Tu, A.-Q. Wang, M.-Y. Zheng, X.-D. Wang, T. Zhang, Factors influencing the catalytic activity of SBA-15-supported copper nanoparticles in CO oxidation, Applied Catalysis A: General, 297 (2006) 40-47.
[27] Z. Xia, H. Liu, H. Lu, Z. Zhang, Y. Chen, High Selectivity of Cyclohexane Dehydrogenation for H2 Evolution Over Cu/SBA-15 Catalyst, Catal. Lett., 147 (2017) 1295-1302.
[28] W. Yin, R. Liu, G. He, W. Lv, H. Zhu, A highly efficient, ligand-free and recyclable SBA-15 supported Cu2O catalyzed cyanation of aryl iodides with potassium hexacyanoferrate(ii), RSC Advances, 4 (2014) 37773-37778.
[29] P.C. Angelomé, M.C. Fuertes, Metal Nanoparticles-Mesoporous Oxide Nanocomposite Thin Films, in: L. Klein, M. Aparicio, A. Jitianu (Eds.) Handbook of Sol-Gel Science and Technology, Springer International Publishing, Cham, 2018, pp. 2507-2533

[30] P.C. Angelomé, L.M. Liz-Marzán, Synthesis and applications of mesoporous nanocomposites containing metal nanoparticles, J. Sol-Gel Sci. Technol., 70 (2014) 180-190.
[31] P. Innocenzi, L. Malfatti, Mesoporous thin films: properties and applications, Chem. Soc. Rev., 42 (2013) 4198-4216.
[32] L. Nicole, C. Boissiere, D. Grosso, A. Quach, C. Sanchez, Mesostructured hybrid organic-inorganic thin films, J. Mater. Chem., 15 (2005) 3598-3627.
[33] M.V. Lombardo, M. Videla, A. Calvo, F.G. Requejo, G. Soler-Illia, Aminopropyl-modified mesoporous silica SBA-15 as recovery agents of Cu (II)-sulfate solutions: Adsorption efficiency, functional stability and reusability aspects, J. Hazard. Mater., 223 (2012) 53-62.
[34] A. Escobar, L. Yate, M. Grzelczak, H. Amenitsch, S.E. Moya, A.V. Bordoni, P.C. Angelomé, One-Step Synthesis of Mesoporous Silica Thin Films Containing Available COOH Groups, ACS Omega, 2 (2017) 4548-4555.
[35] A. Calvo, M. Joselevich, G.J.A.A. Soler-Illia, F.J. Williams, Chemical reactivity of amino-functionalized mesoporous silica thin films obtained by co-condensation and post-grafting routes, Microporous Mesoporous Mater., 121 (2009) 67-72.
[36] C.J. Brinker, Y. Lu, A. Sellinger, H. Fan, Evaporation-induced self-assembly: nanostructures made easy, Adv. Mater., 11 (1999) 579-585.
[37] T.M.D. Dang, T.T.T. Le, E. Fribourg-Blanc, M.C. Dang, Synthesis and optical properties of copper nanoparticles prepared by a chemical reduction method, Advances in Natural Sciences: Nanoscience and Nanotechnology, 2 (2011) 015009.
[38] R. Coneo Rodríguez, M.M. Bruno, P.C. Angelomé, Au nanoparticles embedded in mesoporous ZrO2 films: Multifunctional materials for electrochemical detection, Sens. Actuators, B, 254 (2018) 603-612.
[39] M.M. Zalduendo, J. Langer, J.J. Giner-Casares, E.B. Halac, G.J.A.A. Soler-Illia, L.M. Liz-Marzán, P.C. Angelomé, Au Nanoparticles–Mesoporous TiO2 Thin Films Composites as SERS Sensors: A Systematic Performance Analysis, J. Phys. Chem. C, 122 (2018) 13095-13105.
[40] P.A. DeSario, J.J. Pietron, T.H. Brintlinger, M. McEntee, J.F. Parker, O. Baturina, R.M. Stroud, D.R. Rolison, Oxidation-stable plasmonic copper nanoparticles in photocatalytic TiO2 nanoarchitectures, Nanoscale, 9 (2017) 11720-11729.
[41] P. Liu, H. Wang, X. Li, M. Rui, H. Zeng, Localized surface plasmon resonance of Cu nanoparticles by laser ablation in liquid media, RSC Advances, 5 (2015) 79738-79745.
[42] D. Kim, J. Resasco, Y. Yu, A.M. Asiri, P. Yang, Synergistic geometric and electronic effects for electrochemical reduction of carbon dioxide using gold–copper bimetallic nanoparticles, Nature Communications, 5 (2014) 4948.
[43] D. Mott, J. Galkowski, L. Wang, J. Luo, C.-J. Zhong, Synthesis of size-controlled and shaped copper nanoparticles, Langmuir, 23 (2007) 5740-5745.
[44] C.-F. Hsia, C.-H. Chang, M.H. Huang, Unusually Large Lattice Mismatch-Induced Optical Behaviors of Au@Cu–Cu2O Core–Shell Nanocrystals with Noncentrally Located Cores, Particle & Particle Systems Characterization, 35 (2018) 1800112.
[45] K.P. Rice, E.J. Walker Jr, M.P. Stoykovich, A.E. Saunders, Solvent-dependent surface plasmon response and oxidation of copper nanocrystals, J. Phys. Chem. C, 115 (2011) 1793-1799.
[46] I. Pastoriza-Santos, A. Sánchez-Iglesias, B. Rodríguez-González, L.M. Liz-Marzán, Aerobic Synthesis of Cu Nanoplates with Intense Plasmon Resonances, Small, 5 (2009) 440-443.
[47] A. Marimuthu, J. Zhang, S. Linic, Tuning selectivity in propylene epoxidation by plasmon mediated photo-switching of Cu oxidation state, Science, 339 (2013) 1590-1593.
[48] M.C. Biesinger, L.W.M. Lau, A.R. Gerson, R.S.C. Smart, Resolving surface chemical states in XPS analysis of first row transition metals, oxides and hydroxides: Sc, Ti, V, Cu and Zn, Appl. Surf. Sci., 257 (2010) 887-898.

[49] G. Yang, S. Cheng, C. Li, J. Zhong, C. Ma, Z. Wang, W. Xiang, Investigation of the oxidation states of Cu additive in colored borosilicate glasses by electron energy loss spectroscopy, J. Appl. Phys., 116 (2014) 223707.
[50] R. Leapman, L. Grunes, Anomalous L 3 L 2 White-Line Ratios in the 3 d Transition Metals, Phys. Rev. Lett., 45 (1980) 397.
[51] M. Shi, H.S. Kwon, Z. Peng, A. Elder, H. Yang, Effects of surface chemistry on the generation of reactive oxygen species by copper nanoparticles, ACS Nano, 6 (2012) 2157-2164.
[52] S. Wunder, F. Polzer, Y. Lu, Y. Mei, M. Ballauff, Kinetic analysis of catalytic reduction of 4-nitrophenol by metallic nanoparticles immobilized in spherical polyelectrolyte brushes, J. Phys. Chem. C, 114 (2010) 8814-8820.
[53] B.K. Ghosh, S. Hazra, B. Naik, N.N. Ghosh, Preparation of Cu nanoparticle loaded SBA-15 and their excellent catalytic activity in reduction of variety of dyes, Powder Technol., 269 (2015) 371-378.
[54] I.L. Violi, A. Zelcer, M.M. Bruno, V. Luca, G.J.A.A. Soler-Illia, Gold Nanoparticles Supported in Zirconia–Ceria Mesoporous Thin Films: A Highly Active Reusable Heterogeneous Nanocatalyst, ACS Appl. Mater. Interfaces, 7 (2015) 1114-1121.
[55] P. Zhao, X. Feng, D. Huang, G. Yang, D. Astruc, Basic concepts and recent advances in nitrophenol reduction by gold-and other transition metal nanoparticles, Coordination Chemistry Reviews, 287 (2015) 114-136.
[56] H. Park, D.A. Reddy, Y. Kim, S. Lee, R. Ma, M. Lim, T.K. Kim, Hydrogenation of 4-nitrophenol to 4-aminophenol at room temperature: Boosting palladium nanocrystals efficiency by coupling with copper via liquid phase pulsed laser ablation, Appl. Surf. Sci., 401 (2017) 314-322.
[57] S. Wunder, Y. Lu, M. Albrecht, M. Ballauff, Catalytic activity of faceted gold nanoparticles studied by a model reaction: evidence for substrate-induced surface restructuring, Acs Catalysis, 1 (2011) 908-916.
[58] H. Zhang, N. Toshima, Fabrication of catalytically active AgAu bimetallic nanoparticles by physical mixture of small Au clusters with Ag ions, Applied Catalysis A: General, 447 (2012) 81-88.
[59] C. Kästner, A.F. Thünemann, Catalytic reduction of 4-nitrophenol using silver nanoparticles with adjustable activity, Langmuir, 32 (2016) 7383-7391.
[60] R. Fenger, E. Fertitta, H. Kirmse, A. Thünemann, K. Rademann, Size dependent catalysis with CTAB-stabilized gold nanoparticles, Physical Chemistry Chemical Physics, 14 (2012) 9343-9349.

Synthesis of Cu nanoparticles supported within functional SiO_2 mesoporous films

The functional group (NH_2 or COOH) defines the oxidation state of the Cu particles

Composite's catalytic activity depends on the Cu nanoparticles oxidation state